Analytical Criteria for Stitch Strength of Built-up Compression Members

FARHANG ASLANI and SUBHASH C. GOEL

INTRODUCTION

In the buckled configuration of a built-up compression member, shear force is developed between individual components due to secondary moments caused by P–δ effect. AISC-ASD[1] requires that stitches be designed such that they have adequate strength to resist the shear force developed between individual components. AISC-LRFD[2] also has a similar requirement (see Section E4, p. 6-40). However, neither specification gives a procedure to calculate the shear force developed between individual components in a buckled configuration. This paper presents a derivation of analytical equations to calculate the shear force developed between individual components of built-up struts in buckled configuration. The equations are presented for two cases. First, for the case in which only the first buckling load is of interest. Second, for the case in which, in addition to the first buckling load, post-buckling bending is involved such as in seismic-resistant design. The proposed equations are general enough so that they are applicable to any end condition including the two extreme cases of hinged- and fixed-end conditions.

The proposed equations are verified analytically and experimentally. For analytical verification, the results from the proposed equations are examined for the extreme cases of end conditions and separation between the components. For experimental verification, test results by the authors are used.[3,4] The stitch strength required for some test specimens are calculated according to the proposed equations. The results are compared with actual strength provided by the stitch welds of the corresponding specimens. It was found that specimens which suffered unsymmetrical buckling and/or post-buckling behavior did not have adequate stitch strength according to the proposed equations.

1. NOTATION

Following notations are used in this paper:

- a The distance between batten plates or stitches.
- A_i Cross sectional area of each individual component.
- A Cross sectional area of the member = $2A_i$.
- α Separation ratio = $h / 2r_{ib}$.
- E Young's modulus of elasticity.
- f Lateral deflection at mid-span in buckled configuration (maximum lateral deflection).
- F_S Total shear force developed between individual components.
- F_S^{cr} Total shear force developed between individual components at the time of first buckling.
- F_S^{Pb} Maximum Total shear force developed between individual components in post-buckling range.
- I_{ib} Moment of inertia of individual components about their own centroidal axis parallel to the plane of buckling (y-y axis) = $A_i(r_{ib})^2$
- I_t Moment of inertia of the overall section about the centroidal axis parallel to the plane of buckling (y-y axis).
- K Effective length factor.
- M Moment acting on the member due to P–δ effect.
- M_P Overall plastic moment capacity of the section.
- P Axial compression load sustained by the member.
- P_{cr} Overall buckling load of built-up section.
- Q Maximum static moment of area of the overall section about the centroidal axis parallel to the plane of buckling.
- σ_{cr} Buckling stress.
- σ_p Compression stress in the concave-side component in buckled configuration.
- σ_y Yielding stress of the material.
- τt Shear flow between individual components due to bending in buckled configuration.
- y Lateral deflection of the strut in buckled configuration.

Farhang Aslani is staff engineer, Automated Analysis Corp, Ann Arbor, MI.

Subhash C. Goel is professor of civil engineering, University of Michigan, Ann Arbor, MI.

2. ANALYTICAL CRITERIA FOR STITCH STRENGTH

Analytical equations will be derived for the two cases of hinged- and fixed-end conditions. The result will then be used to develop a single equation which covers general end conditions.

2.1. Hinged-End Conditions

Figure 1 shows the buckling configuration of a hinged-end strut. The total shear force between individual components of a built-up strut is derived in the following. The buckling shape can be represented by:

$$y = f \sin \frac{\pi x}{L} \quad (1)$$

The slope of the buckling shape, y', is given by:

$$y' = \frac{dy}{dx} = \pi \frac{f}{L} \cos \frac{\pi x}{L} \quad (2)$$

The secondary moment in buckled configuration is:

$$M = Py \quad (3)$$

The shear force caused by bending can be expressed by,

$$V = \frac{dM}{dx} = \frac{d(Py)}{dx} = Py' = \pi \frac{f}{L} P \cos \frac{\pi x}{L}$$

The shear flow between individual components is:

$$\tau t = \frac{VQ}{I_t} = \pi \frac{f}{L} \frac{Q}{I_t} P \cos \frac{\pi x}{L} \quad (4)$$

The shear force developed between individual components over the half length can be determined as:

$$\frac{F_s}{2} = \int_0^{L/2} \tau t \, dx = \pi \frac{f}{L} \frac{Q}{I_t} P \int_0^{L/2} \cos \frac{\pi x}{L} dx = \pi \frac{f}{L} \frac{Q}{I_t} P \frac{L}{\pi}$$

or

$$F_s = 2f \frac{Q}{I_t} P \quad (5)$$

a. Consideration of the First Buckling Load

To derive the expression for lateral deflection, f, at the onset of buckling, a procedure similar to that presented by Bleich will be followed (Ref. 5, Eq. 354). In buckled configuration, the total compression stress in the concave side component can be approximated as:

$$\sigma_p = \frac{P_{cr}}{2A_i} + \frac{M / h}{A_i} = \sigma_{cr} + \frac{P_{cr} f}{A_i h}$$

The lateral deflection can be expressed as:

$$f = \frac{\sigma_p - \sigma_{cr}}{P_{cr}} A_i h \quad (6)$$

The above equation gives the lateral deflection at mid-span and is applicable to all struts with any symmetrical end condition. Equation 5 indicates that the amount of shear developed between individual components increases as the lateral deflection increases. If only the first buckling load is of interest, however, it is reasonable to consider the value of f when the stress in concave-side component reaches its maximum value possible, that is the yield stress σ_y. Thus, substitution of σ_y for σ_p in Eq. 6 results in:

$$f = \frac{\sigma_y - \sigma_{cr}}{P_{cr}} A_i h \quad (7)$$

Substituting the above equation into Eq. 5 and replacing P by P_{cr} results in:

$$F_S^{cr} = 2 \frac{\sigma_y - \sigma_{cr}}{P_{cr}} A_i h \frac{Q}{I_t} P_{cr} = 2A_i(\sigma_y - \sigma_{cr}) \frac{Qh}{I_t}$$

$$F_S^{cr} = (P_y - P_{cr}) \frac{Qh}{I_t} \quad (8)$$

Maximum static moment of area is expressed as:

$$Q = A_i h / 2 \quad (9)$$

The total moment of inertia I_t can be written as:

$$I_t = 2I_{ib} + 2[A_i(h/2)^2]$$

Replacing A_i by I_{ib} / r_{ib}^2,

$$I_t = 2I_{ib} + 2\left[\frac{I_{ib}}{r_{ib}^2}(h/2)^2\right] = 2I_{ib}[1 + (h / 2r_{ib})^2]$$

The ratio $h / 2r_{ib}$ is commonly called separation ratio,

$$\alpha = \frac{h}{2r_{ib}}$$

Thus,

$$I_t = 2I_{ib}(1 + \alpha^2) \quad (10)$$

Combining Eqs. 9 and 10, the ratio Qh / I_t can be expressed as:

$$\frac{Qh}{I_t} = \frac{(A_i h / 2)h}{2A_i r_{ib}^2 (1 + \alpha^2)} = \frac{(h / 2r_{ib})^2}{\alpha^2 + 1}$$

Using the definition $\alpha = h / 2r_{ib}$ leads to:

$$\frac{Qh}{I_t} = \frac{\alpha^2}{\alpha^2 + 1} \quad (11)$$

Substitution of Qh / I_t from the above equation into Eq. 8 results in,

$$F_S^{cr} = \frac{\alpha^2}{\alpha^2 + 1} (P_y - P_{cr}) = \frac{\alpha^2}{\alpha^2 + 1} P_y \left(1 - \frac{P_{cr}}{P_y}\right) \quad (12)$$

It should be noted that the above equation gives the total shear force developed between the two individual compo-

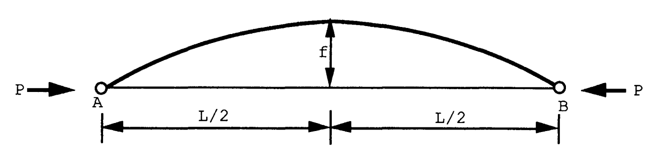

Fig. 1. Symmetric buckling shape of a hinged-end strut.

nents while the distribution of the shear flow shown in Fig. 2. Nonetheless, the stitch strength over the full length must be such that it can resist the total shear force given by Eq. 12.

b. Consideration of Post-Buckling Range

In seismic design, in addition to the first buckling load, the behavior of built-up struts in post-buckling range is of interest as well. In post-buckling range, the value of f exceeds the value associated with yield stress in the concave-side component. According to Eq. 5, shear force developed between the individual components increases as f increases. On the other hand, as the deflection f increases, the axial load sustained by the member decreases. The free body diagram shown in Fig. 3 gives the relationship between the plastic moment capacity of a strut and the axial load sustained by the member. Thus, if conservatively the reduction of plastic moment capacity due to the presence of axial load is neglected, the following equation gives the relationship between f, plastic moment capacity M_p, and sustained axial force P,

$$f = \frac{M_p}{P} \tag{13}$$

Substitution into Eq. 5 results in:

$$F_S^{Pb} = 2\frac{M_p}{P}\frac{Q}{I_t}P = 2M_p\frac{Q}{I_t} \tag{14}$$

From Eq. 11, the ratio Q / I_t can be expressed as:

$$\frac{Q}{I_t} = \frac{\alpha^2}{h(\alpha^2+1)} \tag{15}$$

Substitution of Q / I_t ratio into Eq. 14 leads to:

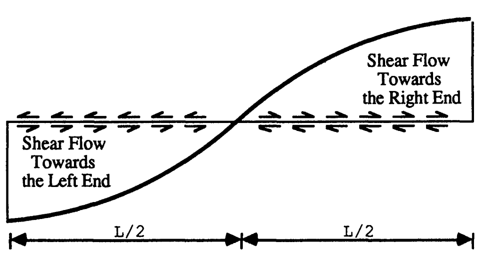

Fig. 2. Shear flow in a hinged-end strut due to secondary moment caused by P–δ effect.

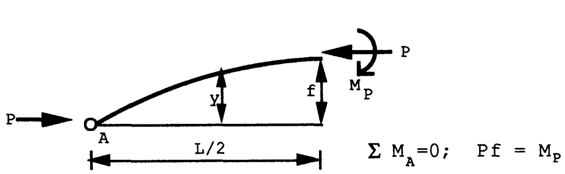

Fig. 3. Free body diagram of a half length hinged-end strut in post-buckling range.

$$F_S^{Pb} = \frac{2\alpha^2}{\alpha^2+1}\frac{M_p}{h} \tag{16}$$

2.2. Fixed-End Conditions

Figure 4a shows the buckling configuration of a fixed-end strut. The total shear force between individual components of a built-up strut can be derived as follows. The buckling shape can be represented by:

$$y = \frac{f}{2}\left(1 - \cos\frac{2\pi x}{L}\right)$$

The above equation satisfies the geometric boundary conditions. The bending moment, denoted by M, is different from that of a hinged-end member, since the end fixity causes non-zero moments at the two ends. The equation for bending moment at a given section is,

$$M = Py + M_e = P\frac{f}{2}\left(1 - \cos\frac{2\pi x}{L}\right) + M_e \tag{17}$$

The term M_e can be determined by basic mechanics approach in which the moment equation is integrated twice to derive the expression for the deflection curve. Then, the boundary conditions are imposed to determine the constants of integration as well as the end moment M_e. Such a procedure results in:

$$M_e = -P\frac{f}{2}$$

Substitution of M_e in Eq. 17 results in:

$$M = P\frac{f}{2}\left(1 - \cos\frac{2\pi x}{L}\right) - P\frac{f}{2} = -P\frac{f}{2}\cos\frac{2\pi x}{L} \tag{18}$$

The above equation gives the moments at the ends and at mid span as:

$$M(x = 0) = -Pf / 2$$

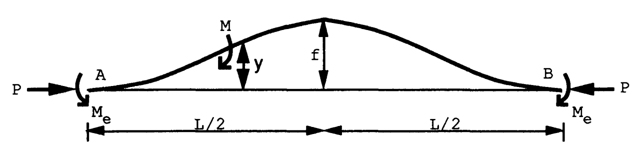

Fig. 4a. Symmetric buckling shape of a fixed-end strut.

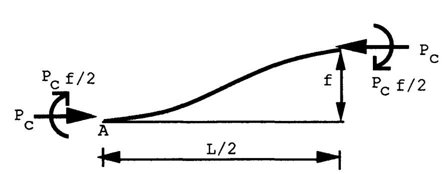

Fig. 4b. Free body diagram of a half length, fixed-end strut after buckling.

$$M(x = L/2) = P\frac{f}{2}(1 - \cos\pi) - Pf/2 = +Pf/2$$

The above two expressions for moment at the ends and at mid-span can be verified by checking the equilibrium equation of the free body diagram shown in Fig. 4b. Therefore, for a fixed-ended strut, the shear force caused by bending is given by:

$$V = \frac{dM}{dx} = \pi\frac{f}{L}P\sin\frac{2\pi x}{L} \tag{19}$$

The shear flow between the two individual components is:

$$\tau t = \frac{VQ}{I_t} = \pi\frac{f}{L}\frac{Q}{I_t}P\sin\frac{2\pi x}{L} \tag{20}$$

The shear force developed between individual components over the half length is:

$$\frac{F_S}{2} = \int_0^{L/2}\tau t\,dx = \pi\frac{f}{L}\frac{Q}{I_t}P\int_0^{L/2}\sin\frac{2\pi x}{L}dx = \pi\frac{f}{L}\frac{Q}{I_t}P\frac{L}{\pi}$$

$$F_S = 2f\frac{Q}{I_t}P \tag{21}$$

It is interesting to note that the above equation is identical to Eq. 5 which was derived for hinged-end case.

a. Consideration of the First Buckling Load

Since Eqs. 5 and 21 are identical, the shear force developed between individual components at the time of the first buckling is identical. Thus,

$$F_S^{cr} = \frac{\alpha^2}{\alpha^2 + 1}P_y\left(1 - \frac{P_{cr}}{P_y}\right) \tag{22}$$

b. Consideration of Post-Buckling Range

For the case in which, in addition to the first buckling load, post-buckling behavior is also of interest, the procedure is different from that of a hinged-end strut only in one step. The difference is that, according to the free body diagram of Fig. 5, the P–δ moment is resisted by $2M_p$ instead of M_p for hinged-end case. Thus,

$$f = \frac{2M_p}{P} \tag{23}$$

Substitution into Eq. 21 results in,

$$F_S^{Pb} = 2\frac{2M_p}{P}\frac{Q}{I_t}P = 4M_p\frac{Q}{I_t}$$

Substituting for Q/I_t from Eq. 15 results in,

$$F_S^{Pb} = \frac{4\alpha^2}{\alpha^2 + 1}\frac{M_p}{h} \tag{24}$$

A comparison between Eqs. 16 and 24 shows that F_S^{Pb} for the fixed-end case is twice of that for hinged-end case.

2.3 General End Conditions

a. Consideration of the First Buckling Load Only

Comparison of Eqs. 12 and 22 shows that end conditions do not change the shear force developed between individual components at the time of first buckling. Thus, for general end conditions the same equation can be used to give the shear force developed between individual components at the time of first buckling.

$$F_S^{cr} = \frac{\alpha^2}{\alpha^2 + 1}P_y\left(1 - \frac{P_{cr}}{P_y}\right) \tag{25}$$

Equation 25 gives the total shear force for which the stitches or batten plates should be designed in order to have a first buckling load identical to that of an integral section with a moment of inertia equal to I_t. It should be noted that Eq. 25 is derived by using an ultimate strength approach which is the basis of AISC-LRFD (1986). Thus, it is convenient to calculate P_{cr} by LRFD formulas and substitute for it in Eq. 25 to find F_S^{cr}. If AISC-ASD formulas are used, the factor of safety should not be included in the calculation of P_{cr}.

b. Consideration of Post-Buckling Range

Comparison of Eqs. 16 and 24 indicates that the two equations are different only by a factor of 2 in the numerator. Thus, for a general end condition, the equation can be given as:

$$F_S^{Pb} = \frac{2\alpha^2}{K(\alpha^2 + 1)}\frac{M_p}{h} \tag{26}$$

Equation 26 gives the total shear force for which the stitches or batten plates may be designed to prevent premature stitch failure which is detrimental to post-buckling behavior. It is recommended that the calculated stitch strength be evenly distributed along the full length of the member in order to prevent possible individual bending of the two components between the stitches. One interesting note about Eq. 26 is that the shear force developed between individual components is linearly proportional to the force M_p/h which, when acting as a couple, applies the moments M_p to the section. The force M_p/h, after being modified by the coefficient of $2\alpha^2/K(\alpha^2 + 1)$, becomes the shear force developed between individual components due to bending.

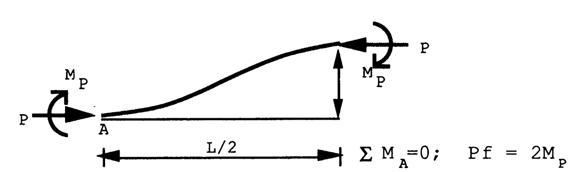

Fig. 5. Free body diagram of a half length, fixed-end strut in post-buckling range.

3. RECOMMENDATIONS FOR STITCH SPACING

Equations 25 and 26 can be used to determine the strength that should be provided by the stitches. Two approaches can be taken as shown in Fig. 6. First, the required strength can be distributed evenly and continuously along the full length of the member, i.e., having a continuous stitch with zero stitch spacing as shown in Fig. 6a. Second, the required strength can be distributed evenly but intermittently along the full length of the member, i.e., having intermittent stitches with a non-zero weld spacing as shown in Fig. 6b. However, previous studies[6,7] indicated that stitch spacing per current code minimum requirement leave boxed angles susceptible to unsymmetric buckling and post-buckling bending mode which result in early failure with much reduced energy dissipation capacity. Furthermore, it was found that smaller stitch spacing in boxed-angles increased the first buckling load and also enhanced the overall member performance due to response closer to that of an integral section. Also, continuous stitch plate significantly enhanced the performance of boxed angles by virtually eliminating section distortion and local buckling, thus, resulting in a much longer fracture life. Generally, for boxed sections made of 2L3×3×⅜-in. double angles as used in the study, a stitch spacing of 12 inches resulted in excellent performance.

Therefore, the required stitch strength according to Eqs. 25 or 26 is recommended to be distributed evenly along the full length of the member.

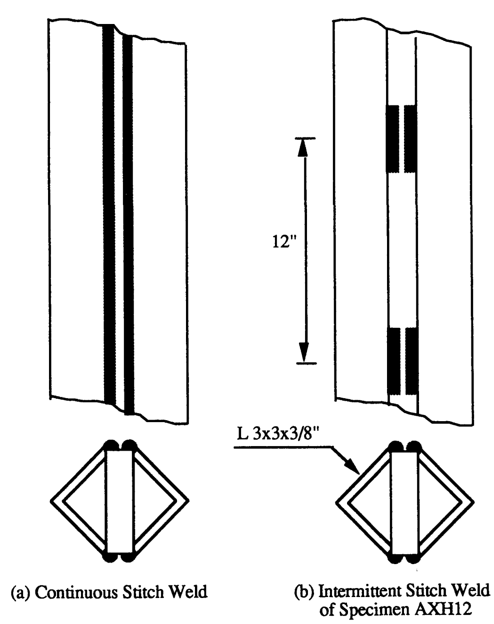

Fig. 6 Continuous and intermittent stitch weld in boxed angles.

4. VERIFICATION OF THE PROPOSED EQUATIONS

4.1. Analytical Verification

Equation 25 gives the total shear force for which the stitches or batten plates can be designed, for the case in which only the first buckling load is of interest. Likewise, Eq. 26 gives the total shear force for which the stitches or batten plates can be designed for the case in which, in addition to the first buckling load, post-buckling behavior is of interest as well. To validate the the proposed equations, the numerical results from these two equations were studied with respect to two parameters, separation ratio and slenderness ratio. The results are discussed in the following two sections.

a. Separation Ratio

Figure 7 shows the variation of the shear force coefficient, C, predicted by Eqs. 25 and 26. The figure also shows two rational results for the two extreme cases of large and zero separation between the two components. First, as separation ratio increases, the coefficient $\alpha^2 / (\alpha^2 + 1)$ approaches its maximum value of 1.0 for which Eqs. 25 and 26 give the maximum shear force. It is reasonable to have large shear force for the cases where the distance between individual components is large. On the other extreme, as separation ratio approaches zero, the coefficient $\alpha^2 / (\alpha^2 + 1)$ approaches zero for which the proposed equations give zero shear force. This is also a reasonable result indicating no shear force for the case where the centroidal axis of the two components coincide with each other. This case, theoretically, is identical to the case of in-plane buckling of a built-up strut in which no shear force is developed between individual components since they are acting in parallel.

b. Slenderness Ratio

A typical column strength curve is shown in Fig. 8. Stocky members with small slenderness ratio buckle inelastically and the buckling load P_{cr} is close to the yield load, P_y. Thus, the coefficient $(1 - P_{cr} / P_y)$ is close to zero. Equation 25 indicates

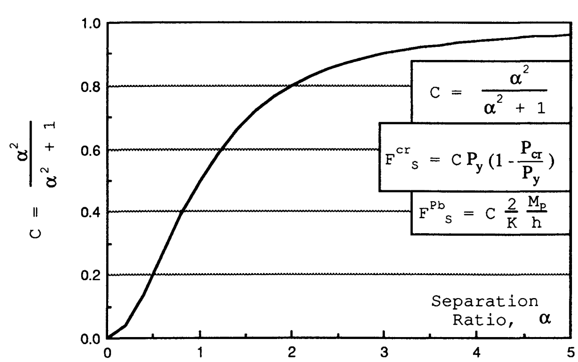

Fig. 7. Variation of shear force coefficient developed between the two components of built-up struts.

Table 1. Geometric Properties of the Test Specimens								
Specimen (1)	End Condition (2)	Section (3)	A (in.^{2}) (4)	$\frac{K_xL}{r_x}$ (5)	$\frac{K_yL}{r_y}$ (6)	Stitch Weld Length (in.) (7)	Number of Stitches (8)	Stitch Plate Spacing (in.) (9)
AB4	Hinged	$2L3.5 \times 2.5 \times 3/8$	4.22	60	95	2	2	37
AXH12		$2L3 \times 3 \times 3/8$		57	83	2	9	0
AXH13						2	2	37
AXFS16	Fixed		6.72	56	58	110	—	0
AXFS17						2	9	0

that a smaller stitch strength is required as the coefficient $(1 - P_{cr} / P_y)$ becomes smaller. This is reasonable since, for stocky members, stability and consequently shear flexibility presents no problem. Instead, yielding is the dominant phenomenon and the member failure is governed by yielding before any buckling occurs.

On the other extreme, Fig. 8 indicates that members with large slenderness ratio buckle elastically and the buckling load P_{cr} is much smaller than the yield load, P_y. Thus, the term $(1 - P_{cr} / P_y)$ is close to 1. Equation 25 indicates that a larger stitch strength is required as the coefficient $(1 - P_{cr} / P_y)$ increases. This is also reasonable since, for slender members, yielding is not involved. Instead, the member failure is governed by elastic buckling. Since buckling load is highly dependant on the buckling shape, the member should have adequate stitch strength to ensure transfer of large shear force between the two components.

4.2. Experimental Verification

Table 1 shows the geometric properties of five specimens from previous experimental study by the authors.[3,4] The stitch strength of these five specimens are checked against those required by the proposed equations. In general, the results show that those specimens, which did not have adequate strength, had unsymmetrical buckling and post-buckling behavior. It should be noted that, in all calculations, the value of P_{cr} / P_y is the one obtained from the corresponding test. However, in a design procedure, the value of P_{cr} / P_y can be calculated by any rational formula. For Specimen AXH12, the detailed calculations according to Eqs. 25 and 26 are presented here. However, the final results for other specimens are summarized in Table 2.

a. Specimen AXH12

Specimen AXH12 had nine 2-in. long ¼-in. stitch welds every 12 inches. For E70 electrodes, the ultimate strength of weld metal in shear is taken as $60 / \sqrt{3}$. If the two end gusset plates are counted as two stitches, the ultimate shear capacity provided by the eleven 2-in. long stitch welds is,

$$R_w = (.707)(1/4)(11 \times 2)\left(\frac{60}{\sqrt{3}}\right) = 135 \text{ kips}$$

The distance between the centroids of the two components is,

$$h = 2[(3\cos 45°) - (0.888 / \cos 45°) + (3/8 \cos 45°)] + 5/8$$
$$= 2.886 \text{ in.}$$

The separation ratio for the section is calculated as:

$$\alpha = \frac{h}{2r_{ib}} = \frac{2.886}{2(0.587)} = 2.46$$

The required shear strength according to Eq. 25 is,

$$F_S^{cr} = \frac{\alpha^2}{\alpha^2 + 1} P_y \left(1 - \frac{P_{cr}}{P_y}\right)$$
$$= \frac{(2.46)^2}{(2.46)^2 + 1}(47 \times 4.22)(1 - 0.94)$$
$$= 10 \text{ kips} < R_w = 135 \text{ kips} \quad \textbf{o.k.}$$

Consistent with the above calculation, no individual component behavior was observed at the first buckling of specimen AXH12. The plastic moment capacity of the section is,

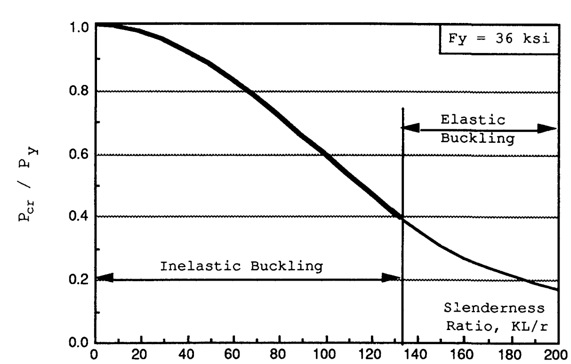

Fig. 8. General column strength curve according to LRFD.[2]

Table 2. Stitch Strength of the Test Specimens								
Specimen (1)	Weld Dimension (in.) (2)	Weld Strength (kips) (3)	Component Separation, h (in.) (4)	Separation Ratio, α (5)	Yield Capacity, P_y (6)	Plastic Moment Capacity, (kip-in.) (7)	F_S^{cr} (Eq. 25) (8)	F_S^{Pb} (Eq. 26) (9)
AXH12	0.25	135	2.886	2.46	198	286	10	170
AXH13	0.25	49			184	266	56	158
AB4	0.25	49	1.950	1.35	198	194	51	128
AXFS16	0.25	673	2.886	2.46	309	447	34	531
AXFS17	0.25	135			312	451	40	536

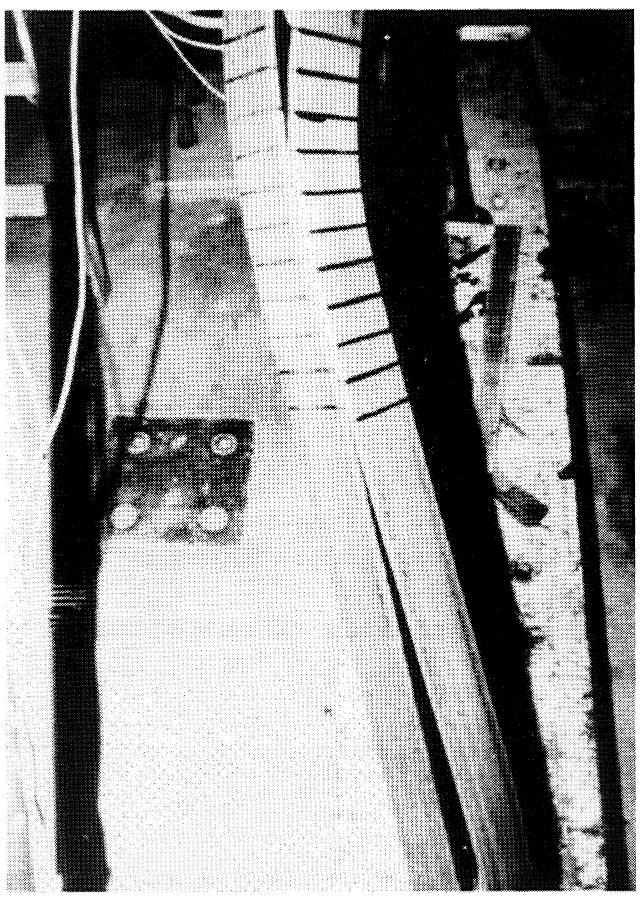

Fig. 9. Unsymmetric buckling of Specimen AXH13.

$$M_p = (A_i F_y)h = 2.11(47)(2.886) = 286 \text{ kip-in.}$$

For the post-buckling range, the required shear strength according to Eq. 26 is,

$$F_S^{Pb} = \frac{2\alpha^2}{K(\alpha^2+1)} \frac{M_p}{h}$$

$$= \left[\frac{2(2.46)^2}{(2.46)^2+1}\right]\left[\frac{286}{2.886}\right]$$

$$= 170 \text{ kips} > R_w = 135 \text{ kips} \quad \textbf{n.g.}$$

However, no individual component behavior or stitch failure occurred in the post-buckling range for this specimen. This may be attributed to the conservative use of unmodified value of the plastic moment capacity M_p, whereas, it may be reduced by about 20 percent due to the presence of axial compression load. If such a reduction in the plastic moment capacity is considered, it follows that,

$$F_S^{Pb} = 80\% \ (170) = 136 \text{ vs. } R_w = 135 \text{ kips} \quad \textbf{almost o.k.}$$

b . Specimen AXH13

Table 1 shows that Specimen AXH13 did not have adequate stitch strength for the first buckling load as well as for the post-buckling range. Consistent with the prediction by Eqs. 25 and 26, individual component bending was observed at the first buckling of specimen AXH13 which caused the occurrence of unsymmetrical buckling mode. The individual bending of the two angle components in Specimen AXH13 is shown in Fig. 9.

c. Specimen AB4

Table 1 indicates that Specimen AB4 had adequate stitch strength for the first buckling load. Consistent with the prediction by Eq. 25, individual bending was not observed at the first buckling of specimen AB4. However, Table 1 shows that the specimen did not have adequate stitch strength for the post-buckling range. Unlike the boxed specimen AXH13, Specimen AB4 did not suffer unsymmetric post-buckling mode. This is attributed to the fact that local buckling is the weakest mode in back-to-back angles. Therefore, local buckling occurs instead of an unsymmetric mode (Aslani and Goel, 1991). In other words, in back-to-back angles with inadequate shear strength which is needed for an integral behavior, the unsymmetric mode is not triggered off since local buckling is the dominant and governing mode. Boxed specimen AXH13, however, had much less potential for local buckling due to its supported edges in the boxed section configuration.

d. Specimen AXFS16

Table 1 indicates that Specimen AXFS16 had adequate stitch strength for the first buckling load as well as for the post-buckling range. Consistent with the prediction by Eqs. 25 and 26, no individual behavior was observed in Specimen AXFS16.

e. Specimen AXFS17

Table 1 indicates that Specimen AXFS17 had adequate stitch strength for the first buckling load. Consistent with the prediction by Eq. 25, individual bending was not observed at the first buckling of specimen AXFS 17. However, Table 1 indicates that the specimen did not have adequate stitch strength for the post-buckling range. Consistent with the prediction by Eq. 26, specimen AXFS 17 suffered stitch failure followed by individual component behavior in the post-buckling range. The shear failure of stitches in Specimen AXFS 17 is shown in Figs. 10 and 11.

CONCLUSIONS

1. Built-up compression members are susceptible to individual behavior of their components. Equation 25 can be used to calculate the required stitch strength to ensure a symmetric first buckling mode.
2. For seismic design, Eq. 26 can be used to calculate the required stitch strength to ensure a symmetric integral behavior in the post-buckling range.

ACKNOWLEDGMENTS

The investigation was sponsored by the National Science Foundation through Grant No. ECE8610963 for which the authors are most grateful. Partial support received from the American Institute of Steel Construction is also acknowledged. The conclusions and opinions expressed in this paper are solely those of the authors and do not necessarily represent the views of the sponsors.

REFERENCES

1. American Institute of Steel Construction, *Steel Construction Manual,* 8th Ed., Chicago, IL, 1980.
2. American Institute of Steel Construction, *Load and Resistance Factor Design,* 1st Ed., Chicago, IL, 1986.
3. Aslani, F. and Goel, S. C., "Stitch Spacing and Local Buckling in Seismic Resistant Double-Angle Braces," Accepted for publication in *Journal of the Structural Division,* ASCE, 1991.
4. Aslani, F., and Goel, S. C., "Experimental and Analytical

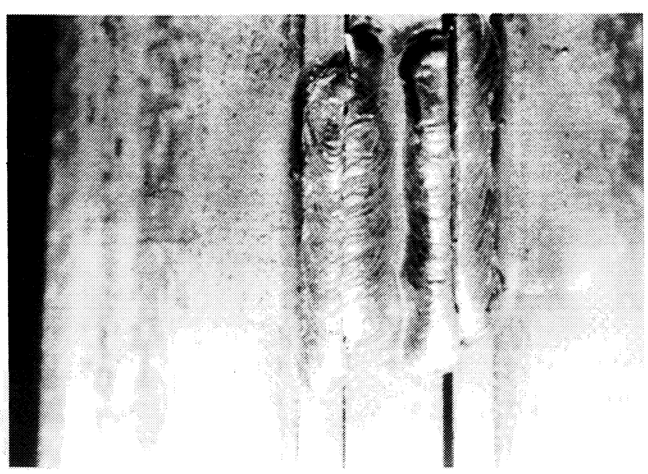

Fig. 10. Shear failure of two stitches in Specimen AXFS17.

Fig. 11. Failure of Specimen AXFS17.

Study of the Inelastic Behavior of Double Angle Bracing Members Under Cyclic Loading," *Report No. UMCE 89-5,* Department of Civil Engineering, University of Michigan, Ann Arbor, Michigan, February 1989.

5. Bleich, F., *Buckling Strength of Metal Structures,* McGraw-Hill Book Company, 1952, pp. 176–179.
6. Aslani, F. and Goel, S. C., "An Analytical Criterion for Buckling Strength of Built-up Compression Members," Submitted for publication in *Engineering Journal,* AISC, 1991.
7. Libove, C., "Sparsely Connected Built-Up Columns," *Journal of the Structural Division,* ASCE, Vol. 111(3), 1985.